

Reactivity of eumelanin building blocks: A DFT study of monomers and dimers

Gabriel G.B. Alves^a, Francisco C. Lavarda^{a, b}, Carlos F.O. Graeff^{a, b}, Augusto Batagin-Neto^{a, c, *}

^a São Paulo State University (UNESP), School of Sciences, Postgraduate Program in Materials Science and Technology (POSMAT), Bauru, 17033-360, Brazil

^b São Paulo State University (UNESP), School of Sciences, Department of Physics, Bauru, 17033-360, Brazil

^c São Paulo State University (UNESP), Campus of Itapeva, Itapeva, 18409-010, Brazil

ARTICLE INFO

Article history:

Received 7 December 2019

Received in revised form

19 February 2020

Accepted 25 March 2020

Available online 8 April 2020

Keywords:

Melanin

Electronic structure calculation

Fukui indexes

Reactivity

ABSTRACT

Melanins are natural pigments with important biological properties and have been considered promising materials for several bio-electronic applications. In spite of it, until now there is no satisfactory understanding of the macromolecular structure of these compounds. In this work, we have employed electronic structure calculations to evaluate the local reactivity on monomeric building blocks of eumelanin and on a varied combination of these units (dimers). The reactivity studies were accomplished by Condensed-to-Atoms Fukui Indexes in a DFT approach. The results have evidenced a dominance order in the reactivity of the building units that guides the polymerization process of melanin. In addition, from the differences of the local reactivities it was possible to better understand the reactions that can take place during eumelanin synthesis and estimate how they could be influenced by experimental conditions.

© 2020 Elsevier Inc. All rights reserved.

1. Introduction

Melanins represent an important class of natural pigments present in plants and animals and have been considered promising materials for technological applications [1–5]. These biological compounds present a series of intriguing properties such as broad-band monotonic absorption, hydrolysis resistance, lack of molecular regularity and paramagnetism [2,5–11]. As a technological material, melanin derivatives can be considered promising organic semiconductors for application in bioelectronics with low environmental impact and low relative cost [2,12,13].

In spite of their interesting opto-electronic properties, until now there is no satisfactory understanding of the macromolecular structure of melanin and its derivatives. In general, there is a consensus in the literature that melanins consist of several redox forms of 5,6-dihydroxyindole (DHI) and 5,6 dihydroxyindole-2-carboxylic acid (DHICA) monomers, but details about the connectivity between these building blocks are still controversial [2,13].

Indeed, the elucidation of the chemical structure of melanin is hindered by the low solubility of this compound that makes the determination of its physical, chemical and structural properties very difficult by traditional spectroscopic techniques [14].

A currently accepted hypothesis describes melanins as a set of stacked planar substructures of DHI and DHICA units (as well as their oxidized counterparts), containing from 4 to 8 monomeric units (proto-molecules) which are aligned along the z axis with inter-planar distances around 3.4 Å [15]. This hypothesis is reinforced by recent studies that show the dominance of smaller structures during melanin synthesis [16]. However the connectivity of the repeating units is still an active research topic.

Studies of oxidative polymerization of 5,6-dihydroxy-indols suggest the formation of different oligomers. Generally oligomers based on DHI structures have connections involving the sites **2**, **3**, **5** and **8** (see Fig. 1), while those based on the DHICA structures are mainly connected via **3**, **5** and **8** positions [16–20]. In particular the existence of dimers **2–2'**, **2–5'**, **2–8'**, **5–5'**, **5–8'** and **8–8'** (the numbers represent the atoms that are connected among monomers M and M') is frequently reported in the literature, however, due to the extremely rich chemistry associated with quinones, other structures may also be formed during the synthesis [16,19,20].

In this study we have employed electronic structure calculations

* Corresponding author. São Paulo State University (UNESP), Campus of Itapeva, Itapeva, 18409-010, Brazil.

E-mail address: a.batagin@unesp.br (A. Batagin-Neto).

to evaluate the reactivity of distinct melanin monomers in water, aiming to investigate details about the connectivity between monomeric units, and to identify the reactions that take place during the synthesis of this biomaterial. Reactivity indexes of selected dimers were also analyzed in order to propose extended structures. The obtained results allow us to evaluate the distribution of reactive sites on the melanin monomers and estimate the relevance of different units in the formation of extended structures of the biomaterial. In particular, nucleating structures and dimerization activation processes were proposed and discussed.

2. Methodology

Fig. 1 shows the basic structures of melanin evaluated in this report.

The ground-state geometries of the monomers were fully optimized in water in a DFT approach with Becke's LYP (B3LYP) [21–24] exchange-correlation functional and 6-31G(2d,p) basis set for the all atoms. Polarizable Continuum Model (PCM) [25,26] was employed to simulate the solvent.

The reactivity studies were accomplished by Condensed-to-Atoms Fukui Indexes (CAFI) [27] obtained via finite difference linearization (FDL) approach [28,29]. In the framework of the conceptual DFT [30,31], these parameters describe the local tendencies of electron releasing/withdrawing on the molecule structure, identifying which sites are prone to undergo reactions with electrophiles, nucleophiles or free radicals [32]. Despite their simplicity, CAFI have been successfully employed to understand and predict local reactivities of molecules and polymers [33–42]. According to the reaction under consideration, three distinct CAFI can be defined [43]:

$$f_k^+ = q_k(N+1) - q_k(N) \quad (1)$$

$$f_k^- = q_k(N) - q_k(N-1) \quad (2)$$

$$f_k^0 = \frac{1}{2} [q_k(N+1) - q_k(N-1)] \quad (3)$$

where $q_k(N+1)$, $q_k(N)$ and $q_k(N-1)$ represent, respectively, the electronic population on the k -th atom of anionic, neutral and cationic configurations of the system under study. f_k^+ , f_k^- and f_k^0 represent, respectively, the plausibility of interactions between the k -th atom of the molecule with electrophiles, nucleophiles or free radicals. CAFI calculations were carried out using the same approach employed for geometry optimizations. Aiming to avoid negative values, Hirshfeld's partition method was employed to estimate the electronic populations [44,45].

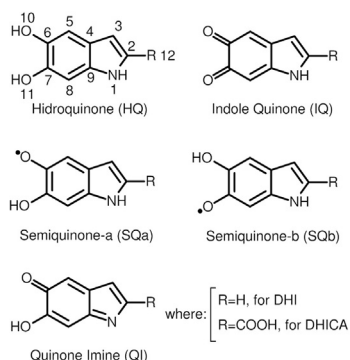


Fig. 1. Monomeric structures of melanin.

In order to evaluate the most likely dimer structures generated during the melanin synthesis, a comparative analysis of the local softness (s_k^+ , s_k^- , and s_k^0) and local philicities (ω_k^+ , ω_k^- , and ω_k^0) [46] were conducted for each structure. These indexes correlates the local information, provided by the CAFI, with the global softness (S) and electrophilicity (ω) [47] of the molecule, allowing to predict the most probable pair of atoms associated with a specific chemical reaction. According to the hard-soft acids-bases (HSAB) principle, the electrophile/nucleophile and radical/radical interactions are favored when the involved atoms present similar softness [27,32,48]. Similarly, a comparative analysis between ω_k^+ , ω_k^- , or ω_k^0 allows the identification of the most plausible sites for intermolecular interactions [49]. In this sense it is possible to propose specific reactions occurring during the synthesis just by comparing these descriptors [38,41,42,49]. Eqs. (4)–(7) illustrate how these parameters were estimated:

$$s_k^n = S \cdot f_k^n, \text{ for } n = (+), (-) \text{ or } (0) \quad (4)$$

$$\omega_k^n = \omega \cdot f_k^n, \text{ for } n = (+), (-) \text{ or } (0) \quad (5)$$

$$S = \frac{1}{IP - EA} \quad (6)$$

$$\omega = \frac{(IP + EA)^2}{8(IP - EA)} \quad (7)$$

where IP represents the ionization potential and EA the electron affinity of the molecule under study, which were estimated by:

$$IP = E(N-1) - E(N) \quad (8)$$

$$EA = E(N) - E(N+1), \quad (9)$$

where $E(M)$ represent the total energy of the compound with M electrons (without geometry relaxation for $M = N+1$ and $M = N-1$).

The analyses of local softness (s_k^n) similarity were carried out by considering reactions involving the most reactive atoms of monomer A (from the CAFIs) and the atoms of monomer B, whose difference in the $s_{i,A}^{n_1}$ (i -th atom of A) and $s_{j,B}^{n_2}$ (j -th atom of B) values did not exceed 5% of $s_{i,A}^{n_1}$, i.e.:

$$\frac{s_{i,A}^{n_1} - s_{j,B}^{n_2}}{s_{i,A}^{n_1}} \leq 0.05. \quad (10)$$

Three cases were considered depending on the nature of n_1 and n_2 : i) $n_1 = (+)$ and $n_2 = (-)$, for reactions involving the i -th atom of A and nucleophilic sites of monomer B; ii) $n_1 = (-)$ and $n_2 = (+)$, for reactions involving the i -th atom of A and electrophilic sites of monomer B; and iii) $n_1 = n_2 = (0)$ for reactions involving free radicals of both the monomers. The similarity value of 5% was chosen to limit the analysis only to the most plausible reactions. A similar work reported by our group has shown that the use of such a matching cutoff is enough to access a significative number of reactions [42]. The same approach was employed for the evaluation of ω_k^n .

To better assess the reactivity of extended structures, CAFI were also calculated for some melanin dimers. Two initial structures were prepared for each dimer, which were differentiated by a rotation of 180° relative to the chemical bond linking the monomeric units (CF₁ and CF₂). The structures were optimized considering water as solvent, via a DFT/B3LYP/6-31G(2d,p)/PCM approach. The CAFI were calculated using the same level of theory and

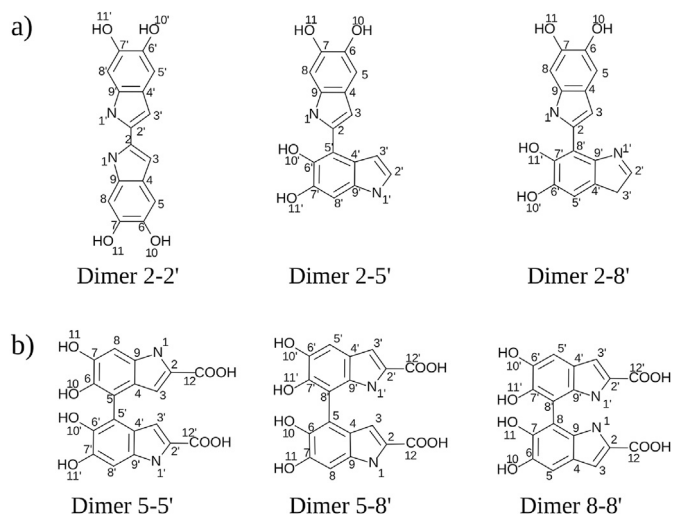


Fig. 2. Structures and numbering employed for melanin dimers: a) DHI and b) DHICA dimers.

approximations presented above. Fig. 2 shows the dimers evaluated as well the atom numbering employed.

For DHICA dimers it was noticed a certain degree of structural degradation after geometry optimization depending on the starting dihedral angles between the monomers, e.g. for $\varphi_D = 0$ and 180° . For this reason these dimeric structures were optimized considering a small increment in these angles.

To analyse the most likely dimers, an energetic analysis of dimerization cost (ΔE_{DC}) was conducted. This evaluation aims to estimate the energy required to produce a dimer from two specific monomers:

$$\Delta E_{DC} = (E_T(\text{dimer AB}) + E_T(H_2)) - E_T(\text{monomer A}) - E_T(\text{monomer B}) \quad (11)$$

where $E_T(X)$ is the total energy of the component X , i.e., the dimer AB, the released hydrogen molecules and the two monomers, A and B, that defines the dimer AB. The values presented in Equation (11) were estimated from single point calculations using the same level of theory employed in the optimization and CAFI calculations.

All the calculations were carried out with the aid of the Gaussian 09 computer package [50]. MOPAC2016 package [51,52] was employed for pre-optimizations, in this case Conductor-like Screening Model (COSMO) was employed to simulate the solvent [53].

3. Results and discussions

3.1. Monomers

Fig. 3 illustrates the results coming from CAFI analyses for DHI and DHICA structures and shows a qualitative representation of the local reactivity on each compound. Red and blue regions represent reactive and non-reactive sites, respectively. The other colors represent sites with intermediate reactivity according to the increasing order: blue, green, yellow, orange, and red (RGB scale). Each molecule has its own color scale to evidence the relative reactivity on the structures (intramolecular analysis). The illustrations were designed with the aid of the Jmol package [54] in conjunction with a specifically developed routine in Fortran 90.

As can be seen, HQ, IQ and QI structures present a number of reactive sites for polymerization, while SQ-based structures

present high reactivity centered only on the “unprotected” quinone oxygens. Despite the qualitative nature of the results presented in Fig. 3, they carry valuable information regarding melanin oligomerization, which can be summarized as follows:

- the high values of f^+ observed on sites 2, 5 and 8 of HQ-DHI are consistent with the position of polymerization sites commonly reported for eumelanin [19,55];
- the high values of f^- on site 2 of HQ-DHI, in conjunction with the above presented results, indicate the plausibility of the formation of the commonly reported dimers 2–2', 2–5' and 2–8';
- the high values of f^- on site 5 and 8 of IQ-DHI, in conjunction with the other results, indicate the formation of dimers 5–5', 5–8' and 2–5', also commonly reported in the literature;
- the high reactivity on the carbon atom of the carboxylic acid in HQ-DHICA structures suggests that this group has a high probability of being removed from the molecule, resulting in a greater proportion of DHI structures in the final material, which is indeed observed in synthetic melanins [8,15,56,57]. On the other hand, the reactivity on this site is reduced for the other DHICA-based structures (IQ, QI and SQ), suggesting that the consumption of DHICA is hindered in the absence of HQ units. This result is consistent with the experimental data reported by Bronze-Uhle et al. which points out that the use of higher oxygen pressures during melanin synthesis lead to materials with an increased amount of carboxylate groups [58]. The high reactivity on the COOH groups obtained for HQ-DHICA structures are also in line with recent studies on the thermal annealing of eumelanin thin films in vacuum [57], in which improved molecular packing and high electronic conductivities were attributed to the removal of labile carboxylic groups.;
- a reduced reactivity is observed towards nucleophiles on sites 5 and 8 of DHICA based structures (f^+). On the other hand, higher values of f^- are observed on these sites, mainly for IQ and QI. In particular the IQ-DHICA present the most relevant results regarding the formation of 5–5', 5–8' and 8–8' connections present in DHICA-rich natural melanins [19,59]. The reduced reactivities on sites 5 and 8 of HQ-DHICA indicate that the synthesis of melanin *in vivo* should involve enzymatic dehydrogenation or H^+ abstraction, which is compatible with the tautomerization of dopachrome into DHICA [60]. Furthermore, the absence of high reactive f^+ sites in DHICA-based structures indicates that 5–5', 5–8' and 8–8' connections, commonly associated with DHICA structures, could indeed be formed with intercalated units of DHI and DHICA subunits, or involve only free-radicals reactions, mainly based on IQ-DHICA;
- the high CAFI values on site 3 of IQ and QI structures, indicate the relevance of these structures for the formation of the commonly reported dimers 3–5' and 3–8' [19];
- the high values of f^- on the lateral oxygens observed for all structures suggest that these sites are susceptible to electrophilic attack, which is compatible with the proposed mechanism of melanin synthesis in DMSO (D-melanin), involving the incorporation of sulfonated groups on these sites [14]. Also, as pointed out by Galvão and Caldas, such sites can be traced as the reason for electron-acceptor properties of melanin units [61];
- regarding D-melanin synthesis, the high reactivity of carbon 2 towards radicals is also compatible with the addition of methyl radicals (arising from the DMSO oxidation process) compatible with an enhanced hydrogen concentration observed in NMR spectra of these materials [14].

In order to evaluate the most likely dimers formed from the interaction between monomers, analyses of the local chemical

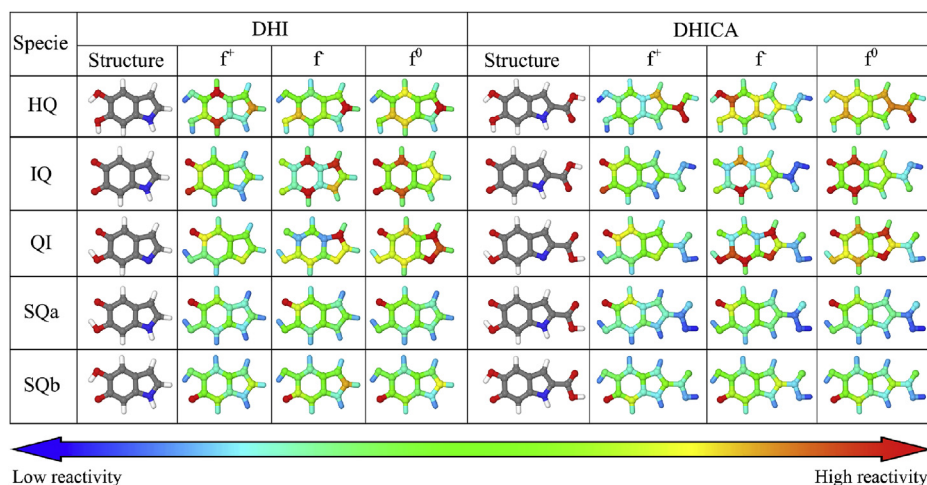


Fig. 3. Condensed-to-atoms Fukui indices obtained for DHI and DHICA monomers.

softness (and local philicities) similarities were carried out. In these analyses the qualitative CAFI indexes are scaled by global parameters of the molecules (chemical softness and electrophilicity), allowing the evaluation of intermolecular interactions. Only reactions involving atoms with high CAFI values were considered. For example, in a reaction involving the monomers A and B, just atoms of A with $f_{k,A}^{n_i} \geq 0.8f_{k,A(max)}^{n_i}$ were considered in the analyses (where $f_{k,A(max)}^{n_i}$ is the highest CAFI value obtained for atom k of monomer A, for a specific reaction $n_i = +, -, \text{ or } 0$, identified by the red regions in Fig. 3), and their local softness and philicities were compared in relation to all the atoms of monomer B for an appropriate reaction. Tables 1–3 present the most probable combinations of atoms for each type of reaction between the monomers A and B. The analyses of local softness and local philicities lead to the same interactions

(see Supplementary material for details). Asterisks identify the most plausible connections that do not involve internal/protected regions, which are indeed expected in the real systems.

It is worth mentioning that the combinations presented in Tables 1–3 were taken from simple numeric comparisons, that do not take into account the surrounding atoms, free-valences and the plausibility of molecular rearrangements, in this sense, some of the connections in these tables are indeed non-realistic. For instance, given steric hindrance and stability effects, the connections involving the atoms 4, 9 and 12 are not supposed to occur. Reactions involving the atoms 6 and 7, which require the removal of the OH groups can also be considered very unlikely [62]. The connections involving atoms 1, 10, 11, 13 and 14, should generate very unstable structures that are supposed to break up during the synthesis

Table 1
Analysis of the softness matching considering the atoms of monomer A as electrophiles and the atoms of monomer B as nucleophiles (evaluation of s_A^+ and s_B^-).

Monomer A	i-th atom of A	Monomer B (j-th atom of B)									
		HQ		IQ		QI		SQa		SQb	
		DHI	DHICA	DHI	DHICA	DHI	DHICA	DHI	DHICA	DHI	DHICA
HQ-DHI	8	–	–	10,11	–	–	–	4,7	9,6	1,4,9	6,1
	5*	–	–	11	–	–	–	3*,4,7	9,1	1,4	4
	2	–	–	–	–	–	–	–	2	6	9,14
HQ-DHICA	3*	2*	–	10	10	–	2	–	6	9	9,6,14
	12	–	10	–	5	–	–	–	–	–	–
	14	–	10	–	–	–	–	–	2	–	–
IQ-DHI	8*	–	–	2*	–	–	–	2*	10	3*,7	7,10
	2*	–	–	2*	–	–	–	2*,6,11	7,10	3*,7	7,2,10
	11	–	–	–	3	8,11	–	5	–	–	–
IQ-DHICA	10	–	–	1	3	8,2	11	5	8	–	–
	5	–	–	–	–	11	–	6,11	7,10	–	2,10
	10	–	–	–	3	8,2,11	–	5	–	–	–
QI-DHI	11	–	–	–	–	–	–	6,11	7,10	7	2,10
	5*	–	–	–	3*	8*,2*,11	–	5*	–	–	–
	2*	–	–	–	–	–	–	6,11	7,10	3*,7	2,7,10
QI-DHICA	10	–	–	1	3	8,2	11	5	8	–	–
	5*	–	–	1	3*	8*,2*	11	5*	8*	–	–
	10	–	–	–	3	8,2,11	–	5	–	–	–
SQa-DHI	5*	–	–	–	8*	3*	–	–	–	–	–
SQb-DHI	2*	–	–	–	–	3*	–	–	–	–	–
	8*	–	–	8*	–	3*	–	–	–	–	–
	11	–	–	–	8	–	–	–	–	2	–
SQb-DHICA	8*	–	–	–	8*	3*	–	–	–	2*	–
	11	–	–	–	8	–	–	–	–	2	–

Table 2Analysis of the softness matching considering the atoms of monomer A as nucleophiles and atoms of monomer B as electrophiles (evaluation of s_A^- and s_B^+).

Monomer A	i-th atom of A	Monomer B (j-th atom of B)									
		HQ		IQ		QI		SQa		SQb	
		DHI	DHICA	DHI	DHICA	DHI	DHICA	DHI	DHICA	DHI	DHICA
HQ-DHI	2*	2*	–	–	–	–	7,2	4	7	1,6	6,1,14
HQ-DHICA	10	–	–	6	2	6	6	–	4,2	9	–
	11	8,5	–	–	7	9	9	–	–	–	9
IQ-DHI	5*	–	–	–	–	–	–	5*	–	8*	–
	8*	–	–	–	–	–	–	5*	5*	8*	8*
	3*	–	–	–	–	–	–	5*	–	8*	–
	1	–	–	5,8	8,5	3	–	–	–	–	–
IQ-DHICA	8*	–	–	–	–	–	–	10	10	2*,11	11
	5*	–	–	–	–	–	–	5*	–	8*	–
QI-DHI	3*	–	–	–	–	–	–	10	5*	2*,11	8*,11
QI-DHICA	8*	–	–	–	8*	–	–	5*	–	–	–
	3*	–	–	–	8*	–	–	–	–	–	–
	11	–	–	5,8	8,5	3	–	–	–	–	–
SQa-DHI	5*	–	–	5*,8*	5*	3*	–	–	–	–	–
	10	–	–	–	–	–	–	5	–	8	8
SQa-DHICA	5*	–	–	5*,8*	8*,5*	3*	–	–	–	–	–
	10	–	–	–	–	–	–	5	–	8	–
SQb-DHI	2*	–	–	–	–	–	–	10	10	2*	–
	11	–	–	–	–	–	–	5	–	8	–
SQb-DHICA	8*	–	–	–	–	–	–	5*	–	8*	–
	11	–	–	–	–	–	–	5	–	8	–

Table 3Analysis of the softness matching considering the atoms of monomer A and B as radicals (evaluation of s_A^0 and s_B^0).

Monomer A	i-th atom of A	Monomer B (j-th atom of B)									
		HQ		IQ		QI		SQa		SQb	
		DHI	DHICA	DHI	DHICA	DHI	DHICA	DHI	DHICA	DHI	DHICA
HQ-DHI	8*	5*,8*	–	7	6,7	9	9	–	–	–	9
	5*	5*,8*	–	–	7	9	9	–	–	–	9
	2*	2*	–	–	–	7	7,2	4	7	9,6	6,14
HQ-DHICA	5*	–	5*,14	9	9	–	4	–	–	–	12
	3*	–	3*	4	–	–	–	–	–	–	13
	14	3	5,14	9	9	–	–	–	14	–	12
IQ-DHI	5*	–	–	5*,8*	5*	3*	–	–	–	–	–
	8*	–	–	5*,8*	5*	3*	–	–	–	–	–
	3*	–	–	2*,3*	–	8*,5*	8*,5*	2*,11	–	–	2,10
	2*	–	–	2*,3*	–	8*,5*	8*,5*	2*,11	–	–	2,10
IQ-DHICA	8*	–	–	–	8*,5*	–	–	–	–	–	–
	5*	–	–	5*,8*	8*,5*	3*	–	–	–	–	–
QI-DHI	8*	–	–	2*,3*,10,11	11	8*,5*	8*,5*	2*,6,11	6	3*,10	2,10
	5*	–	–	2*,3*	–	8*,5*	8*,5*	2*,11	–	–	2
	3*	–	–	5*,8*	5*	3*	–	–	–	–	–
	2*	–	–	–	–	2*	3*	–	–	–	–
QI-DHICA	8*	–	–	2*,3*	–	8*,5*	8*,5*	2*,11	–	–	2
	5*	–	–	2*,3*	–	8*,5*	8*,5*	11	–	–	2
	3*	–	–	–	–	2*	3*	–	–	–	–
	11	–	–	10,11	3,10,11	1,11	11	6	6,11	3,7,10	7
SQa-DHI	1	–	–	–	–	–	–	5	–	–	–
	10	–	–	–	–	–	–	10	–	8	11
SQa-DHICA	2	–	–	–	–	–	–	10	–	–	2
	8*	–	–	–	–	–	–	5*	10	2*	8*
SQb-DHI	2	–	–	–	–	–	–	10	–	11	11
	8*	–	–	–	–	–	–	5*	10	–	–
	16	–	–	–	–	–	–	10	–	–	8,11
SQb-DHICA	8*	–	–	–	–	–	–	–	5*	11	8*,11
	11	–	–	–	–	–	–	10	10	2,11	8,11

process. However, it is interesting to highlight that some structures coming from the dimerization via unprotected oxygens have some similarity with the oligomeric structures proposed by Nicolaus [63]. Connections via N-hydrogen substitution in general requires quite aggressive conditions [64–68] which are not compatible with the

natural and synthetic routes employed in melanin synthesis, and then are not supposed to occur.

In general, it is noticed that the plausible interactions (labeled by asterisks in Tables 1–3) involve distinct monomers. Especially, it is noticed that the formation of hydrogenated structures (HQHQ) is

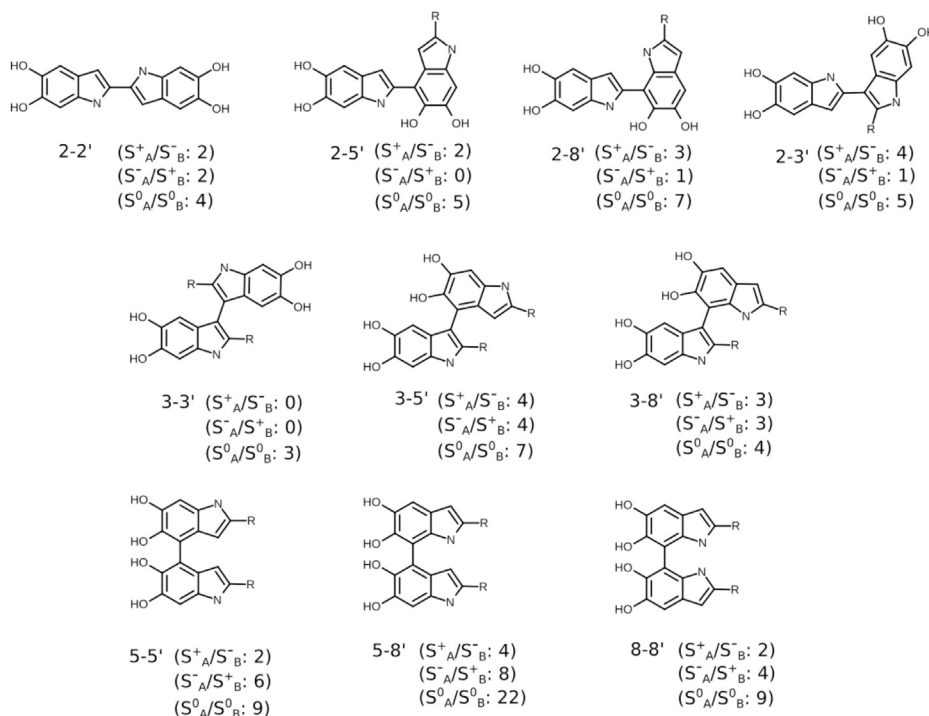


Fig. 4. Most probable dimeric structures coming from HSAB principle analysis.

very unlikely, which is consistent with the fact that melanin derivatives must be synthesized in slightly alkaline solutions. As a matter of fact, a variety of plausible connections are observed for IQ, QI and SQ units, suggesting that they play a nucleating role in melanin polymerization. In particular, IQ and QI present the most relevant (plausible) interactions.

From Tables 1–3 note that the formation of DHICA-DHICA structures in general do not involve electron transfer processes (electrophilic/nucleophilic reactions) which are commonly observed for DHI-DHI and DHI-DHICA dimers. This result is in agreement with the fact that spontaneous oxidation of DHICA is generally much slower than DHI, mainly due to the inductive effect of COOH group [17]. In addition, it is also in line with the work of Okuda et al. that have described electron-transfer-controlled reactions in DHI oligomerization [18].

Fig. 4 summarizes the most likely dimeric structures obtained from the analysis of Tables 1–3, as well as the number of occurrences observed for each kind of reaction. The above mentioned chemically unstable and/or unlikely structures were omitted for simplicity.

In fact, all these dimeric structures have been reported in the literature [16]. A relevant feature is the high plausibility of 5–8', 5–5', 8–8', 3–5', and 3–8' structures in relation 2-X'-based ones, which are mainly associated with free radical reactions. Considering that 5-X' and 8-X' connections are mainly associated with DHICA-based oligomers, while 2–5' and 2–2' are mainly associated with DHI structures [19], our results suggest that DHICA oligomerization are mainly governed by radical reactions while DHI polymerization is also associated with charge transfer processes.

Indeed, it is well known that the oxidation of DHICA units is essentially an enzymatic reaction, however, details regarding the exact mechanisms associated are still unknown [20]. Recent results have indicated that the synthesis of melanin under (varied) O_2 positive pressure induces the formation of carboxylated materials [58]. Our results suggest that such conditions could facilitate the

formation of active units (IQ, QI or SQ) for melanin formation [69], at the same time that prevents the removal of COOH groups, that are very reactive in HQ structures.

In addition, the results presented in Tables 1–3 are compatible with those reported by Chen and Buehler [55], in which 72 dimeric structures (obtained via a brute-force algorithm and optimized via an *ab-initio* approach) were employed to define the most stable dimers of eumelanin (DHI and its reduced forms).

3.2. Dimers

To better access the reactivity patterns on larger structures of melanin, the CAFIs were also evaluated for dimers 2–2', 2–5' and 2–8' for DHI and 5–5', 5–8' and 8–8' for DHICA. All these structures have been widely reported in the literature, and were also identified as the most likely structures in this work. Two distinct conformations were considered for each dimer, according to the dihedral angle (φ_D) between monomer blocks: i) conformer **01** (CF₁) with $\varphi_D = 0^\circ$ and ii) conformer **02** (CF₂) with $\varphi_D = 180^\circ$.

Fig. 5 presents the results obtained for the conformers **02** of the dimers 2–2'. The color scheme is the same employed in Fig. 3. Similar results were obtained for conformers CF₁ (see Supplementary Material for details).

In order to shorten the discussions, let us divide our considerations in homo-structured dimers (HoSD): HQHQ, IQIQ, QIQI and SQSQ, and hetero-structured dimers (HeSD). We will also limit our discussion only to the parameters f^+ and f^- , since f^0 is the average of these values.

For 2–2'/HQHQ, a high reactivity is observed on sites 3 and 3', suggesting that the presence of such structures in the reaction medium can lead to the formation of oligomers based on 3-X' connections. High reactivity is also observed on sites 2 and 2', which suggests that these dimers could be fragmented during the synthesis or degradation of melanin. As a matter of fact, metallic cations are required to generate 2–2' dimers during the oxidation

Species	Structure	f^+	f^-	f^0	Species	Structure	f^+	f^-	f^0
HQHQ					IQIQ				
HQIQ					IQQI				
HQQI					IQSQa				
HQSQa					SQaSQa				
QIQI					QISQa				

Fig. 5. Fukui indexes calculated for dimers 2–2'.

of L-DOPA [13,18,19]. Such metal centers could act as chelating agents on the quinone oxygens (susceptible to interaction with electrophiles), changing the electron density on the 2–2' bond of these dimers (stabilizing them) and facilitating their observation in the final products. In addition, it can be noticed that the dominance of f^- indexes in relation to f^+ (evidenced in f^0) for HQ-X dimers suggests that HQ based materials indeed acts as good electron-donor materials, as has reported elsewhere [61].

For dimers 2–2'/IQQ, 2–2'/QIQI, and 2–2'/SQaSQa it is noticed that more reactive sites are located on the unprotected oxygens, similarly to the monomers. In all of these structures it is also observed the activation of sites 3 and/or 5.

In general, for all the dimers it is noticed the following order of dominance in relation to the monomer reactivity: HQ < IQ ~ QI ≤ SQa, in other words, the reactivity features of SQa prevail in relation to the other units for all the dimers, while the features associated with HQ are less expressive. In particular, the f^+ indexes of the HeSD follow the same tendencies of the monomers (according to

the dominance order above described). In relation to f^- , the activation of sites 3 and/or 8 is observed for most of the structures, with exception to SQ-based dimers, in which high reactivity is noticed only on the unprotected oxygens.

Fig. 6 illustrates the CFI obtained for 2–5' dimers. As previously, red and blue regions represents, respectively, sites with high and low reactivity.

For dimer 2–5'/HoSD, note that the addition of a second unit on site 5' increases the reactivity on sites 3 and 8'. Such a result suggests that the formation of this dimer leads to tetramers based on 8'–X" connections typically proposed for DHI-based eumelanins [70]. The high reactivity noticed on site 3 could lead to the formation of extended structures based on 3–X" connections also reported in the literature [17,56]. In particular, for IQ, QI and SQa, the unprotected oxygens have also significant reactivity.

Similarly to 2–2', the reactivity of the connected units is: HQ < IQ ~ QI ≤ SQa. For instance, in the 2–5'/HeSD HQIQ the unit IQ dominates the overall reactivity of the structure. In general, the f^+

Species	Structure	f^+	f^-	f^0	Species	Structure	f^+	f^-	f^0
HQHQ					IQHQ				
HQIQ					IQIQ				
HQQI					IQQI				
HQSQa					IQSQa				
QIHQ					SQaHQ				
QIIQ					SQaIQ				
QIQI					SQaQI				
QISQa					SQaSQa				

Fig. 6. Fukui indexes calculated for the dimers 2–5'.

Species	Structure	f^+	f^-	f^0	Species	Structure	f^+	f^-	f^0
HQHQ					IQHQ				
HQIQ					IQIQ				
HQQI					IQQI				
HQSQa					IQSQa				
QIHQ					SQaHQ				
QIIQ					SQaIQ				
QIQI					SQaQI				
QISQa					SQaSQa				

Fig. 7. Fukui indexes calculated for dimers 2–8'.

indexes of the dimer are quite similar to the f^+ values of the dominant monomer. Such tendency was also noticed for some IQ and QI based structures in relation to f^- (IQQI and QIIQ). For the other structures the index f^- present some relevant changes: i) activation of site 8 in HQIQ; ii) activation of site 2 in HQQI; iii) activation of sites 3 and 5 in IQSQa, QISQa, and SQaSQa. In particular, the dimers IQIQ and IQQI present high reactivity on sites 3 and 5 (for f^- and f^0) that could lead to extended structures (trimer, tetramers, etc) based on 3–X'' and 5–X'' connections (where X'' represents the active site of another melanin subunit).

Fig. 7 illustrates the CAFI obtained for 2–8' dimers.

The same tendencies discussed for dimers 2–5' are observed in dimers 2–8' with few exceptions, mainly related to f^- indexes: i) the high reactivities on sites 2' are not observed in HQQI and QIQI; ii) site 8 that was not active in 2–5' is activated in HQSQa; iii) an increase in the reactivity of sites 3 and 5 are noticed for QISQa and SQaSQa; and iv) a reduction of the reactivities on sites 3 and 5 for

IQHQ. The changes on f^+ parameter were less expressive, being limited to deactivation of sites 3 and 5 in QISQa and activation of site 8 in SQaSQa. As noticed for 2–2', 2–5' and 2–8', the dimers IQIQ and IQQI show a significant reactivity on sites 3 and 5 (and 8 for IQQI).

Figs. 8 and 9 illustrate the CAFI obtained for 5–5' and 8–8' dimers. Given the symmetry of these dimers, only 10 structures are presented instead of the usual 16 (mainly due to the HoSD).

Generally the highest reactivities on 5–5' dimers are found on the positions 8 and/or 8' for HQ, IQ, and QI based structures and 3 (and/or 3') for QI ones. High reactivities are also observed on the unprotected oxygens of SQa-based dimers. HQ, IQ and QI based structures present some reactivity on the sterically protected sites (2, 4, 7 and 9) and on position 3. The reactivity is similar to those already discussed for the DHI-based dimers (HQ < IQ ~ QI ≤ SQa). The same tendencies are observed for dimers 8–8', with high reactivity on sites 5 and 5'.

Species	Structure	f^+	f^-	f^0	Species	Structure	f^+	f^-	f^0
HQHQ					IQIQ				
HQIQ					IQQI				
HQQI					IQSQa				
HQSQa					SQaSQa				
QIQI					QISQa				

Fig. 8. Fukui indexes calculated for dimers 5–5'.

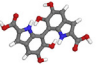
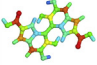
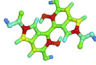
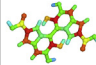
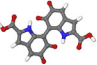
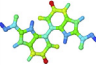
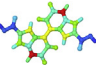
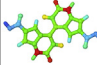
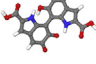
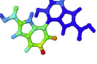
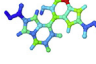
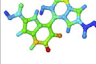
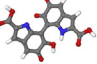
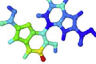
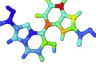
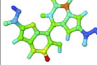
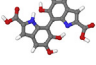
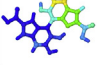
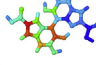
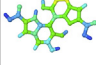
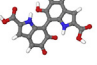
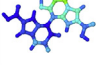
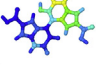
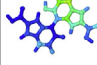
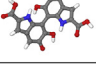
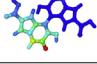
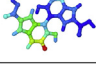
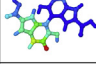
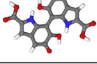
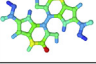
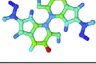
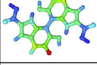
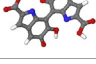
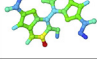
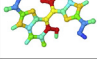
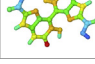
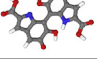
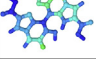
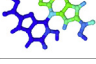
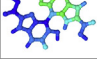
Species	Structure	f ⁺	f ⁻	f ⁰	Species	Structure	f ⁺	f ⁻	f ⁰
HQHQ					IQIQ				
HQIQ					IQQI				
HQQI					IQSQa				
HQSQa					SQaSQa				
QIQI					QISQa				

Fig. 9. Fukui indexes calculated for dimers 8–8'.

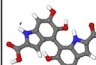
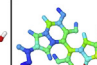
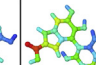
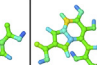
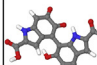
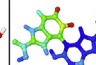
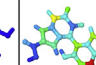
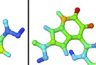
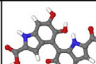
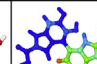
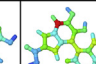
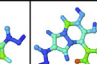
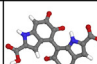
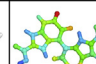
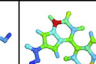
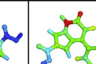
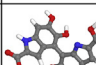
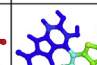
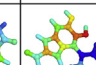
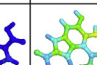
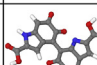
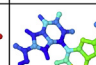
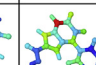
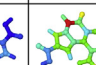
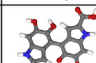
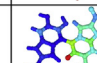
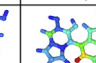
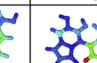
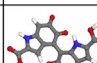
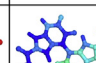
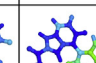
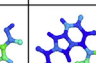
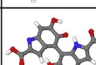
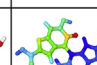
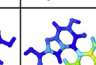
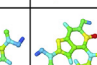
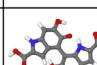
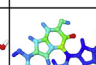
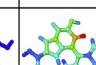
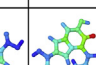
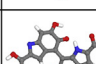
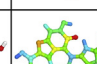
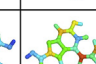
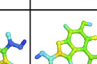
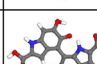
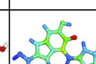
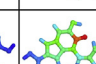
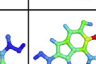
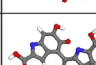
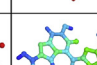
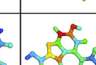
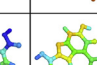
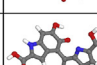
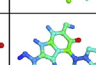
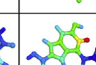
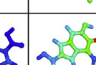
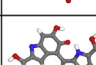
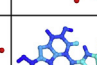
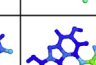
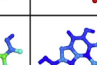
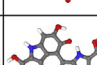
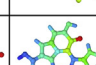
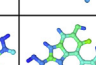
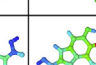
Species	Structure	f ⁺	f ⁻	f ⁰	Species	Structure	f ⁺	f ⁻	f ⁰
HQHQ					IQHQ				
HQIQ					IQIQ				
HQQI					IQQI				
HQSQa					IQSQa				
QIHQ					SQaHQ				
QIIQ					SQaIQ				
QIQI					SQaQI				
QISQa					SQaSQa				

Fig. 10. Fukui indexes calculated for dimers 5–8'.

In both cases, activation of sites 5 (5') and/or 8 (8') highlights the relevance of IQ units in the formation of 5–5', 5–8', and 8–8' connections, which are widely reported for DHICA-based structures. The results also suggest that QI units are responsible for the formation of 3–8', 3–5' and 3–3' connections, also observed in natural melanins. These results are in line with those obtained for the monomers.

Fig. 10 illustrates CFI obtained for 5–8' dimers. As previously, red and blue regions represents sites with high and low reactivity, respectively.

As can be seen, 5–8' HoSD present high reactivity on non-connected 5 and 8 sites. High reactivity at sites 3 and 3' are also observed for the QIQI dimer, which is in agreement with the formation of 3–5' and 3–8' structures, already reported in the literature [71]. SQaSQa structures do not present relevant reactivities.

For the HeSD, one of the monomers dominates the reactivity following the same order as previously presented: HQ < IQ ~ QI ≤ SQa. Activation of sites 5 and 8 is noticed in dimers containing IQ units, except in cases where the SQa unit is present (in particular it is observed that the QI monomer activates the 5 and 8 positions in SQa-based dimers). This result reinforces the relevance of IQ units in the synthesis of extended structures of DHICA-melanins, which was already observed in the study of monomers.

Based on CFI results, the following points can be summarized: i) there is a great variety of reactive sites in the different monomeric and dimeric units of melanin building blocks; ii) the reactivity dominance of the units in the dimers is given by: HQ < IQ ~ QI ≤ SQa; this sequence can also be present in more extended structures and dictate the oligomerization process; iii) the IQ and QI structures play a key role in melanin oligomerization, leading to the activation

ΔE_{DC} (eV)

Dimer	DHI						DHICA						
	2-2'		2-5'		2-8'		5-5'		8-8'		5-8'		
	CF ₁	CF ₂	CF ₁	CF ₂	CF ₁	CF ₂	CF ₁	CF ₂	CF ₁	CF ₂	CF ₁	CF ₂	
HQHQ	0.511	0.436	0.652	0.576	0.404	0.440	0.660	0.659	0.591	0.596	0.574	0.472	1.742
HQIQ	0.373	0.285	0.595	0.430	0.421	0.292	0.596	0.599	0.456	0.569	0.569	0.605	1.621
HQQI	0.440	0.396	0.607	0.538	0.216	0.301	0.553	0.564	0.526	0.420	0.651	0.482	1.501
HQSQa	0.825	0.715	0.784	0.563	0.514	0.427	0.599	0.592	0.559	0.641	0.617	0.639	1.380
IQHQ	0.373	0.285	0.472	0.435	0.376	0.400	0.596	0.599	0.596	0.569	0.608	0.604	1.259
IQIQ	0.637	0.535	0.536	0.443	0.405	0.279	0.578	0.568	0.610	0.511	0.551	0.590	1.139
IQQI	0.626	0.497	0.493	0.453	0.240	0.344	0.584	0.578	0.581	0.600	0.627	0.620	1.018
IQSQa	0.756	0.640	0.698	0.511	0.417	0.343	0.508	0.489	0.611	0.517	0.564	0.596	0.897
QIHQ	0.440	0.396	0.622	0.843	0.262	-0.068	0.553	0.564	0.526	0.420	0.617	0.532	0.777
QIIQ	0.626	0.497	0.559	0.612	0.013	0.394	0.584	0.578	0.581	0.600	0.559	0.581	0.656
QIQI	0.008	0.217	0.827	1.097	0.459	0.400	0.652	0.658	0.668	0.668	0.633	0.630	0.535
QISQa	1.080	1.034	0.662	0.975	0.065	0.373	0.507	0.496	0.599	0.613	0.585	0.596	0.415
SQaHQ	0.825	0.715	0.964	0.833	0.431	0.441	0.599	0.592	0.559	0.641	0.542	0.361	0.294
SQaIQ	0.756	0.640	0.360	0.222	0.410	0.249	0.508	0.489	0.611	0.517	0.434	0.522	0.173
SQaQI	1.080	1.034	0.997	0.874	0.181	0.275	0.506	0.496	0.599	0.613	0.572	0.572	0.053
SQaSQa	0.407	0.482	1.742	1.371	0.324	0.947	0.475	0.414	1.331	1.213	1.032	1.143	-0.068

Fig. 11. Representation of the energetic costs for dimer formation associated with DHI and DHICA-based systems.

of positions 5/8 and site 3, respectively; iv) a secondary role is assigned to SQ and HQ units.

In addition to CAFI results, another important point to consider is the energy required for the dimers formation (dimerization costs, ΔE_{DC}). Fig. 11 represents a color map of the ΔE_{DC} values estimated for each dimeric structure in a red-white-blue scale (red > white > blue). The structures XY and YX (where X,Y= HQ, IQ, QI or SQa) of the symmetric dimers 2-2', 5-5' and 8-8' present the same ΔE_{DC} values.

In relation to DHI, it is possible to identify the dimer 2-8' as the most likely structure, mainly those containing QI units. In general it is noticed the following order of energetic costs for DHI dimers formation: 2-8' < 2-2' < 2-5'. Higher costs are observed for species containing SQa units. Regarding DHICA, it is observed similar costs for the varied structures, so that a very heterogeneous material is expected. It is also noticed that SQa-based structures are stabilized in relation to DHI, mainly for 5-5' dimers, which could be linked with the superior free-radical-scavenging properties of DHICA [59]. The higher dimerization costs of DHICA-based structures in relation to DHI ones are also compatible with their low concentration in synthetic melanins, evidencing the relevance of enzymatic process for their formation [8].

4. Conclusions

The reactivity and structural features of melanin monomers and dimers were evaluated by electronic structure calculations.

By analyzing the reactivity and local softness of the monomers, it was possible to identify the position of the most reactive sites of the distinct species HQ, IQ, QI, and SQ and evaluate the most likely nucleophilic, electrophilic and radical reactions that may occur during melanin synthesis process.

It has been observed that the synthesis of DHI-based materials must be controlled by charge transfer reactions, while DHICA-based eumelanins are mainly associated with radical reactions.

Different dimeric structures were then proposed and discussed.

The indices obtained in the monomers study is compatible with the mechanism proposed for the synthesis of melanin derivatives in DMSO (D-melanins), indicating the incorporation of sulfonated groups on the oxygens.

In the dimers, the reactivity dominance order of the units is given by: HQ < IQ ~ QI ≤ SQ. IQ and QI monomers play a relevant role in the dimerization reactions. In general, the presence of IQ units leads to the activation of sites 5 and 8, so that the X-IQ dimers (DHI and DHICA) are important polymerization centers. The presence of QI units activates the site 3.

In addition to melanins, the results presented here can be extended to other highly complex macromolecules in order to help elucidate possible synthesis routes and polymerization processes [42].

Data availability

The data that support the findings of this study are available from the corresponding author upon request.

Declaration of competing interest

The authors declare no conflict of interest.

Acknowledgments

The authors thank the Brazilian agencies FAPESP (grants 2012/03116-7 and 2013/07296-2), CNPq (grants 448310/2014-7 and 420449/2018-3) and CAPES/PROEX (grant 88882.330142/2019-01) for the financial support. This research was also supported by resources supplied by the Center for Scientific Computing (NCC/GridUNESP) of São Paulo State University (UNESP).

Appendix A. Supplementary data

Supplementary data to this article can be found online at <https://doi.org/10.1016/j.jmngm.2020.107609>.

References

- [1] M. Piacenti da Silva, J.C. Fernandes, N.B. de Figueiredo, M. Congiu, M. Mulato, C.F.O. Graeff, Melanin as an active layer in biosensors, *AIP Adv.* 4 (3) (2014), <https://doi.org/10.1063/1.4869638>, 037120.
- [2] P. Meredith, K. Tandy, A.B. Mostert, A hybrid ionic-electronic conductor: melanin, the first organic amorphous semiconductor? in: F. Cicoira, C. Santato (Eds.), *Organic Electronics Wiley-VCH Verlag GmbH & Co. KGaA*, 2013, pp. 91–111.
- [3] J. Wünsche, L. Cardenas, F. Rosei, F. Cicoira, R. Gauvin, C.F.O. Graeff, S. Poulin, A. Pezzella, C. Santato, Bioelectronics: in situ formation of dendrites in eumelanin thin films between gold electrodes (adv. Funct. Mater. 45/2013), *Adv. Funct. Mater.* 23 (45) (2013), <https://doi.org/10.1002/adfm.201370229>, 5569–5569.
- [4] F. Cicoira, C. Santato (Eds.), *Organic Electronics: Emerging Concepts and Technologies, first ed.*, Wiley-VCH, Weinheim, 2013.
- [5] A. Antidormi, C. Melis, E. Canadell, L. Colombo, Assessing the performance of eumelanin/Si interface for photovoltaic applications, *J. Phys. Chem. C* 121 (21) (2017) 11576–11584, <https://doi.org/10.1021/acs.jpcc.7b02970>.
- [6] M. Blois, A. Zahlan, J. Maling, Electron spin resonance studies on melanin, *Biophys. J.* 4 (6) (1964) 471–490, [https://doi.org/10.1016/S0006-3495\(64\)86797-7](https://doi.org/10.1016/S0006-3495(64)86797-7).
- [7] P.J. Gonçalves, O.B. Filho, C.F.O. Graeff, Effects of hydrogen on the electronic properties of synthetic melanin, *J. Appl. Phys.* 99 (10) (2006), <https://doi.org/10.1063/1.2201691>, 104701–104701–5.
- [8] P. Meredith, T. Sarna, The physical and chemical properties of eumelanin, *Pigm. Cell Res.* 19 (6) (2006) 572–594, <https://doi.org/10.1111/j.1600-0749.2006.00345.x>.
- [9] T. Sarna, H.A. Swartz, The physical properties of melanins, in: J.J. Nordlund, R.E. Boissy, V.J. Hearing, R.A. King, W.S. Oetting, J.-P. Ortonne (Eds.), *The Pigmentary System*, Blackwell Publishing Ltd, 2006, pp. 311–341.
- [10] A. Batagin-Neto, E.S. Bronze-Uhle, C.F.O. Graeff, Electronic structure calculations of ESR parameters of melanin units, *Phys. Chem. Phys.* 17 (11) (2015) 7264–7274, <https://doi.org/10.1039/C4CP05256K>.
- [11] J.V. Paulin, A. Batagin-Neto, C.F.O. Graeff, Identification of common resonant lines in the EPR spectra of melanins, *J. Phys. Chem. B* 123 (6) (2019) 1248–1255, <https://doi.org/10.1021/acs.jpcc.8b09694>.
- [12] A.B. Mostert, B.J. Powell, I.R. Gentle, P. Meredith, On the origin of electrical conductivity in the bio-electronic material melanin, *Appl. Phys. Lett.* 100 (9) (2012), <https://doi.org/10.1063/1.3688491>, 093701.
- [13] M. d'Ischia, A. Napolitano, A. Pezzella, P. Meredith, T. Sarna, Chemical and structural diversity in eumelanins: unexplored bio-optoelectronic materials, *Angew. Chem. Int. Ed.* 48 (22) (2009) 3914–3921, <https://doi.org/10.1002/anie.200803786>.
- [14] E.S. Bronze-Uhle, A. Batagin-Neto, P.H. Xavier, N.I. Fernandes, E.R. de Azevedo, C.F. Graeff, Synthesis and characterization of melanin in DMSO, *J. Mol. Struct.* 1047 (2013) 102–108, <https://doi.org/10.1016/j.molstruc.2013.04.061>.
- [15] G. Zajac, J. Gallas, J. Cheng, M. Eisner, S. Moss, A. Alvarado-Swaigood, The fundamental unit of synthetic melanin: a verification by tunneling microscopy of X-ray scattering results, *Biochim. Biophys. Acta Gen. Subj.* 1199 (3) (1994) 271–278, [https://doi.org/10.1016/0304-4165\(94\)90006-X](https://doi.org/10.1016/0304-4165(94)90006-X).
- [16] A. Antidormi, C. Melis, E. Canadell, L. Colombo, Understanding the polymerization process of eumelanin by computer simulations, *J. Phys. Chem. C* 122 (49) (2018) 28368–28374, <https://doi.org/10.1021/acs.jpcc.8b09484>.
- [17] J. Borovanský, P.A. Riley, Melanins and Melanosomes: Biosynthesis, Structure, Physiological and Pathological Functions, John Wiley & Sons, 2011.
- [18] H. Okuda, K. Wakamatsu, S. Ito, T. Sota, Possible oxidative polymerization mechanism of 5,6-dihydroxyindole from ab initio calculations, *J. Phys. Chem. A* 112 (44) (2008) 11213–11222, <https://doi.org/10.1021/jp711025m>.
- [19] S. Ito, K. Wakamatsu, M. D'Ischia, A. Napolitano, A. Pezzella, Structure of melanins, in: J. Borovanský, P.A. Riley (Eds.), *Melanins and Melanosomes*, Wiley-VCH Verlag GmbH & Co. KGaA, 2011, pp. 167–185. <http://onlinelibrary.wiley.com/doi/10.1002/9783527636150.ch6/summary>.
- [20] J.C. García-Borrón, M.C. Olivares Sánchez, Biosynthesis of melanins, in: J. Borovanský, P.A. Riley (Eds.), *Melanins and Melanosomes*, Wiley-VCH Verlag GmbH & Co. KGaA, 2011, pp. 87–116.
- [21] A.D. Becke, Density-functional thermochemistry. III. The role of exact exchange, *J. Chem. Phys.* 98 (7) (1993) 5648–5652, <https://doi.org/10.1063/1.464913>.
- [22] C. Lee, W. Yang, R.G. Parr, Development of the Colle-Salvetti correlation-energy formula into a functional of the electron density, *Phys. Rev. B* 37 (2) (1988) 785–789, <https://doi.org/10.1103/PhysRevB.37.785>.
- [23] S.H. Vosko, L. Wilk, M. Nusair, Accurate spin-dependent electron liquid correlation energies for local spin density calculations: a critical analysis, *Can. J. Phys.* 58 (8) (1980) 1200–1211, <https://doi.org/10.1139/p80-159>.
- [24] P.J. Stephens, F.J. Devlin, C.F. Chabalowski, M.J. Frisch, Ab initio calculation of vibrational absorption and circular dichroism spectra using density functional force fields, *J. Phys. Chem.* 98 (45) (1994) 11623–11627, <https://doi.org/10.1021/j100096a001>.
- [25] F. Jensen, *Introduction to Computational Chemistry*, second ed., John Wiley & Sons, Chichester, England ; Hoboken, NJ, 2007.
- [26] I.N. Levine, *Quantum Chemistry*, fifth ed., Prentice Hall, 1999.
- [27] W. Yang, W.J. Mortier, The use of global and local molecular parameters for the analysis of the gas-phase basicity of amines, *J. Am. Chem. Soc.* 108 (19) (1986) 5708–5711, <https://doi.org/10.1021/ja00279a008>.
- [28] F. Zielinski, V. Tognetti, L. Joubert, Condensed descriptors for reactivity: a methodological study, *Chem. Phys. Lett.* 527 (2012) 67–72, <https://doi.org/10.1016/j.cplett.2012.01.011>.
- [29] H. Chermette, Chemical reactivity indexes in density functional theory, *J. Comput. Chem.* 20 (1) (1999) 129–154, [https://doi.org/10.1002/\(SICI\)1096-987X\(19990115\)20:1<129::AID-JCC13>3.0.CO;2-A](https://doi.org/10.1002/(SICI)1096-987X(19990115)20:1<129::AID-JCC13>3.0.CO;2-A).
- [30] P. Geerlings, F. De Proft, W. Langenaeker, Conceptual density functional theory, *Chem. Rev.* 103 (5) (2003) 1793–1874, <https://doi.org/10.1021/cr990029p>.
- [31] L. Domingo, M. Ríos-Gutiérrez, P. Pérez, Applications of the conceptual density functional theory indices to organic chemistry reactivity, *Molecules* 21 (6) (2016) 748, <https://doi.org/10.3390/molecules21060748>.
- [32] E.G. Lewars, *Computational Chemistry: Introduction to the Theory and Applications of Molecular and Quantum Mechanics*, second ed., Springer, 2010.
- [33] T. Mineva, Selectivity study from the density functional local reactivity indices, *J. Mol. Struct.: THEOCHEM* 762 (1–3) (2006) 79–86, <https://doi.org/10.1016/j.theochem.2005.08.044>.
- [34] J. Cruz, L.M.R. Martínez-Aguilera, R. Salcedo, M. Castro, Reactivity properties of derivatives of 2-imidazoline: an ab initio DFT study, *Int. J. Quant. Chem.* 85 (4–5) (2001) 546–556, <https://doi.org/10.1002/qua.10018>.
- [35] E.S. Bronze-Uhle, A. Batagin-Neto, F.C. Lavarada, C.F.O. Graeff, Ionizing radiation induced degradation of poly (2-methoxy-5-(2'-ethyl-hexyloxy) -1,4-phenylene vinylene) in solution, *J. Appl. Phys.* 110 (7) (2011), <https://doi.org/10.1063/1.3644946>, 073510.
- [36] A. Batagin-Neto, E.S. Bronze-Uhle, M.G. Vismara, A.P. Assis, F. Castro, T. Geiger, F.C. Lavarada, C.F.O. Graeff, Gamma-Ray dosimetric properties of conjugated polymers in solution, *Curr. Phys. Chem.* 3 (4) (2013) 431–440, <https://doi.org/10.2174/18779468113036660026>.
- [37] I. Cesarino, R.P. Simões, F.C. Lavarada, A. Batagin-Neto, Electrochemical oxidation of sulfamethazine on a glassy carbon electrode modified with graphene and gold nanoparticles, *Electrochim. Acta* 192 (2016) 8–14, <https://doi.org/10.1016/j.electacta.2016.01.178>.
- [38] L.M. Martins, S. de Faria Vieira, G.B. Baldacim, B.A. Bregadiolli, J.C. Caraschi, A. Batagin-Neto, L.C. da Silva-Filho, Improved synthesis of tetraaryl-1,4-dihydropyrrrolo[3,2-b]pyrroles a promising dye for organic electronic devices: an experimental and theoretical approach, *Dyes Pigments* 148 (2018) 81–90, <https://doi.org/10.1016/j.dyepig.2017.08.056>.
- [39] J. do Amaral Rodrigues, A.R. de Araújo, N.A. Pitombeira, A. Plácido, M.P. de Almeida, L.M.C. Veras, C. Delerue-Matos, F.C.D.A. Lima, A. Batagin-Neto, R.C.M. de Paula, J.P.A. Feitosa, P. Eaton, J.R.S.A. Leite, D.A. da Silva, Acetylated cashew gum-based nanoparticles for the incorporation of alkaloid epipilopturine, *Int. J. Biol. Macromol.* 128 (2019) 965–972, <https://doi.org/10.1016/j.ijbiomac.2019.01.206>.
- [40] L. O. Mandú, A. Batagin-Neto, Chemical sensors based on N-substituted polyaniline derivatives: reactivity and adsorption studies via electronic structure calculations, *J. Mol. Model.* 24 (7). doi:10.1007/s00894-018-3660-5.
- [41] A. Rodrigues de Araújo, B. Iles, K. de Melo Nogueira, J.N. Dias, A. Plácido, A. Rodrigues, P. Albuquerque, I. Silva-Pereira, R. Sododatto, C.C. Portugal, J.B. Relvas, L.M. Costa Veras, F.C. Dalmatti Alves Lima, A. Batagin-Neto, J.-V. Rolim Medeiros, P.H. Moreira Nunes, P. Eaton, J.R. de Souza de Almeida Leite, Antifungal and anti-inflammatory potential of eschweilenol C-rich fraction derived from Terminalia gaffigolia Mart, *J. Ethnopharmacol.* 240 (2019) 111941, <https://doi.org/10.1016/j.jep.2019.111941>.
- [42] R.A. Maia, G. Ventorim, A. Batagin-Neto, Reactivity of lignin subunits: the influence of dehydrogenation and formation of dimeric structures, *J. Mol. Model.* 25 (8) (2019) 228, <https://doi.org/10.1007/s00894-019-4130-4>.
- [43] R.G. Parr, W. Yang, Density functional approach to the frontier-electron theory of chemical reactivity, *J. Am. Chem. Soc.* 106 (14) (1984) 4049–4050, <https://doi.org/10.1021/ja00326a036>.
- [44] F. De Proft, C. Van Alsenoy, A. Peeters, W. Langenaeker, P. Geerlings, Atomic charges, dipole moments, and Fukui functions using the Hirshfeld partitioning of the electron density, *J. Comput. Chem.* 23 (12) (2002) 1198–1209, <https://doi.org/10.1002/jcc.10067>.
- [45] R.K. Roy, S. Pal, K. Hirao, On non-negativity of Fukui function indices, *J. Chem. Phys.* 110 (17) (1999) 8236–8245, <https://doi.org/10.1063/1.478792>.
- [46] P.K. Chattaraj, B. Maiti, U. Sarkar, Philicity: a unified treatment of chemical reactivity and selectivity, *J. Phys. Chem.* 107 (25) (2003) 4973–4975, <https://doi.org/10.1021/jp034707u>.
- [47] R.G. Parr, L.v. Szentpály, S. Liu, Electrophilicity index, *J. Am. Chem. Soc.* 121 (9) (1999) 1922–1924, <https://doi.org/10.1021/ja983494x>.
- [48] R.G. Parr, W. Yang, *Density-functional Theory of Atoms and Molecules*, Oxford University Press, 1994.
- [49] P.K. Chattaraj, U. Sarkar, D.R. Roy, Electrophilicity index, *Chem. Rev.* 106 (6) (2006) 2065–2091, <https://doi.org/10.1021/cr040109f>.
- [50] M.J. Frisch, G.W. Trucks, H.B. Schlegel, G.E. Scuseria, M.A. Robb, J.R. Cheeseman, G. Scalmani, V. Barone, B. Mennucci, G.A. Petersson, H. Nakatsuji, *Gaussian 09*, 2009.
- [51] J.J.P. Stewart, MOPAC, A semiempirical molecular orbital program, *J. Comput.*

- Aided Mol. Des. 4 (1) (1990) 1–103, <https://doi.org/10.1007/BF00128336>.
- [52] J.J.P. Stewart, MOPAC2016. <http://OpenMOPAC.net>, 2018.
- [53] A. Klamt, G. Schuurmann, COSMO: a new approach to dielectric screening in solvents with explicit expressions for the screening energy and its gradient, *J. Chem. Soc. Perkin Trans. 2* (5) (1993) 799–805, <https://doi.org/10.1039/P29930000799>.
- [54] A. Herráez, How to Use Jmol to Study and Present Molecular Structures, Lulu.com, Morrisville, NC, 2007.
- [55] C.-T. Chen, M.J. Buehler, Polydopamine and eumelanin models in various oxidation states, *Phys. Chem. Chem. Phys.* 20 (44) (2018) 28135–28143, <https://doi.org/10.1039/C8CP05037F>.
- [56] G.A. Swan, A. Waggott, Studies related to the chemistry of melanins. Part X. Quantitative assessment of different types of units present in dopa-melanin, *J. Chem. Soc. C* 10 (1970) 1409, <https://doi.org/10.1039/j39700001409>.
- [57] L. Migliaccio, P. Manini, D. Altamura, C. Giannini, P. Tassini, M.G. Maglione, C. Minarini, A. Pezzella, Evidence of unprecedented high electronic conductivity in mammalian pigment based eumelanin thin films after thermal annealing in vacuum, *Front. Chem.* 7 (2019) 162, <https://doi.org/10.3389/fchem.2019.00162>.
- [58] E.S. Bronze-Uhle, J.V. Paulin, M. Piacenti-Silva, C. Battocchio, M.L.M. Rocco, C.F.O. Graeff, Melanin synthesis under oxygen pressure: melanin synthesis under oxygen pressure, *Polym. Int.* 65 (11) (2016) 1339–1346, <https://doi.org/10.1002/pi.5185>.
- [59] L. Panzella, G. Gentile, G. D'Errico, N.F. Della-Vecchia, M.E. Errico, A. Napolitano, C. Carfagna, M. d'Ischia, Atypical structural and π -electron features of a melanin polymer that lead to superior free-radical-scavenging properties, *Angew. Chem. Int. Ed.* 52 (48) (2013) 12684–12687, <https://doi.org/10.1002/anie.201305747>.
- [60] J.L. Muñoz-Munoz, F. García-Molina, R. Varón, J. Tudela, F. García-Cánovas, J.N. Rodríguez-López, Generation of hydrogen peroxide in the melanin biosynthesis pathway, *Biochim. Biophys. Acta Protein Proteomics* 1794 (7) (2009) 1017–1029, <https://doi.org/10.1016/j.bbapap.2009.04.002>.
- [61] D.S. Galvão, M.J. Caldas, Theoretical investigation of model polymers for eumelanins. I. Finite and infinite polymers, *J. Chem. Phys.* 92 (4) (1990) 2630, <https://doi.org/10.1063/1.457957>.
- [62] F.A. Carey, *Organic Chemistry*, eighth ed., McGraw-Hill, New York, 2011.
- [63] M.S. Blois, Random polymer as a matrix for chemical evolution, in: *The Origins of Prebiological Systems and of Their Molecular Matrices*, Academic Press, 1965, pp. 19–33.
- [64] J.A. Joule, K. Mills, *Heterocyclic Chemistry*, fifth ed., Wiley, Hoboken, NJ, 2009.
- [65] S.T. Hilton, K. Jones, T.C.T. Ho, G. Pljevaljic, M. Schulte, A tandem radical approach to the ABCE-rings of the Aspidosperma and Strychnos alkaloids, *Chem. Commun.* (2) (2001) 209–210, <https://doi.org/10.1039/b008465o>.
- [66] C. Tratrat, S. Giorgi-Renault, H.-P. Husson, Oxidative cleavage of indole π -lactones with *m*-chloroperbenzoic acid: first synthesis of spiroindolin-2-one-lactones, *J. Org. Chem.* 65 (20) (2000) 6773–6776, <https://doi.org/10.1021/jo000694u>.
- [67] O. Ottoni, R. Cruz, R. Alves, Efficient and simple methods for the introduction of the sulfonyl, acyl and alkyl protecting groups on the nitrogen of indole and its derivatives, *Tetrahedron* 54 (46) (1998) 13915–13928, [https://doi.org/10.1016/S0040-4020\(98\)00865-5](https://doi.org/10.1016/S0040-4020(98)00865-5).
- [68] Y.R. Jorapur, J.M. Jeong, D.Y. Chi, Potassium carbonate as a base for the *N*-alkylation of indole and pyrrole in ionic liquids, *Tetrahedron Lett.* 47 (14) (2006) 2435–2438, <https://doi.org/10.1016/j.tetlet.2006.01.129>.
- [69] E. S. Bronze-Uhle, M. Piacenti-Silva, J. V. Paulin, C. Battocchio, C. F. O. Graeff, Synthesis of Water-Soluble Melanin, arXiv:1508.07457 [cond-mat].
- [70] A. Pezzella, L. Panzella, A. Natangelo, M. Arzillo, A. Napolitano, M. d'Ischia, 5,6-Dihydroxyindole tetramers with "anomalous" interunit bonding patterns by oxidative coupling of 5,5',6,6'-Tetrahydroxy-2,7'-biindolyl: emerging complexities on the way toward an improved model of eumelanin buildup, *J. Org. Chem.* 72 (24) (2007) 9225–9230, <https://doi.org/10.1021/jo701652y>.
- [71] A. Pezzella, A. Napolitano, M. d'Ischia, G. Prota, Oxidative polymerisation of 5,6-dihydroxyindole-2-carboxylic acid to melanin: a new insight, *Tetrahedron* 52 (23) (1996) 7913–7920, [https://doi.org/10.1016/0040-4020\(96\)00362-6](https://doi.org/10.1016/0040-4020(96)00362-6).